Tingting Liu, Xuping Su, Ya Liu, Changjun Wu and Jianhua Wang*

Microstructural Evolution of Aluminum Alloy 2618 During Homogenization and Its Kinetic Analysis

Abstract: The microstructure evolution of aluminum alloy 2618 and its homogenization kinetics were investigated by optical microscope, scanning electron microscope, energy dispersive spectroscopy and differential scanning calorimeter. The results show that the main constituent phases in as-cast alloy 2618 are α–Al, Al_9FeNi phase and non-equilibrium binary θ (Al_2Cu) phase instead of typical S (Al_2CuMg) phase. The θ phase was dissolved into α–Al gradually and the continuous dendritic-network structure was broken with the increase of homogenization temperature and time. DSC analysis shows that the overburnt and liquidus temperatures of as-cast alloy 2618 are 506.4 °C and 638.0 °C, respectively. After the alloy was homogenized at optimized temperature 500 °C for 16 h, the θ phase was completely dissolved in matrix. The size and morphology of Al_9FeNi phase had little change, while the liquidus temperature shifted to 641 °C. The calculated homogenization time for alloy 2618 at 500 °C is 15 h, which is in accordance with that obtained in homogenization experiments.

Keywords: 2618 alloy, non-equilibrium, homogenization, overburnt, kinetic equation

PACS® (2010). 81.05.Bx

***Corresponding author: Jianhua Wang:** School of Materials Science and Engineering, Changzhou University, Changzhou, Jiangsu 213164, China; Key Laboratory of Advanced Metallic Materials of Changzhou City, Changzhou University, Changzhou, Jiangsu 213164, China. E-mail: wangjh@cczu.edu.cn

Tingting Liu, Xuping Su, Ya Liu, Changjun Wu: School of Materials Science and Engineering, Changzhou University, Changzhou, Jiangsu 213164, China; Key Laboratory of Advanced Metallic Materials of Changzhou City, Changzhou University, Changzhou, Jiangsu 213164, China

1 Introduction

Heat treatable aluminum alloy 2618 (AA2618) is an Al-Cu-Mg-Fe-Ni forging alloy developed for aircraft engine components and automobile industries and has good elevated temperature strength up to 238 °C derived from a combination of precipitation and dispersion hardening [1–3]. Compared with other 2000 series aluminum alloys, the mechanical properties of alloy 2618 at both ambient and elevated temperatures are improved due to the precipitation of Guinier-Preston-Bagaryatskii (GPB) (Cu, Mg) zones during aging at temperature up to at least 200 °C and the formation of semi-coherent S′(Al_2CuMg) phase as well as the stable intermetallic particles of the Al_9FeNi phase [4, 5]. Moreover, wrought alloy 2618 fabricated by ingot metallurgy (IM) method is much cheaper than Al-Fe-Si-V series alloys produced by rapid solidification (RS) [6, 7]. But after a long-term exposure to elevated temperature up to 300 °C, the mechanical properties of alloy 2618 are inferior to that of Al-Fe-Si-V series alloys owing to coarsening of fine precipitation particles which are the effective strengthening source [8, 9]. In recent years, a lot of researches [10–15] have been done to improve the mechanical properties of alloy 2618 by alloying and heat treatment, etc.

The mechanical properties of alloys largely depend on their original ingot structure, heat treatment and subsequent deformation conditions, etc. [16]. Microsegregation and inhomogeneities would be accompanied with normal ingot solidification due to fast cooling in conventional DC (direct-chill) casting. Thus it is necessary to add energy to the solid metal in the method of heat treatment to obtain homogeneity which is strongly dependent on the distribution of alloying elements, as are the properties of the final materials [17, 18]. Before hot rolling or extrusion, homogenization treatment is carried out directly after alloy casting, which plays a crucial role in dissolving soluble non-equilibrium eutectic phases and eliminating microsegregation [19]. The effect of homogenization on microstructure and properties of aluminum alloys have been reported by many researchers [16, 19–21]. But up till now, there are few studies on the homogenization of alloy 2618, which are of great importance to the improvement of its deformation and mechanical properties.

The microstructural evolution of alloy 2618 and its homogenization kinetic of the alloy has been investigated in present study. The obtained results can give useful information for optimizing actual homogenization processing parameters in industry.

Table 1: Chemical compositions of experimental alloys (mass fraction, %).

	Cu	Mg	Fe	Ni	Si	Mn	Al
Composition range	1.9~2.5	1.4~1.8	1.0~1.5	1.0~1.5	<0.35	<0.2	Bal.
Designed composition	2.3	1.6	1.1	1.1	<0.35	<0.2	Bal.
Measured composition	2.3	1.5	1.0	1.0	<0.35	<0.2	Bal.

2 Experimental

The specified composition range of alloy 2618, designed and measured compositions of the casting alloy are provided in Table 1. The used materials are industrial pure Al (99.7 mass%), Al-50 mass% Cu, Al-25 mass% Mg, Al-10 mass% Fe and Al-10 mass% Ni master alloys. The alloy was melted and refined in graphite crucible which was heated in electrical resistance furnace. Then the liquid alloy was poured at 670 °C into a preheated steel mould (100 °C) with the inner size of $100 \times 50 \times 15$ mm. The casting ingots were cut into the specimens with a dimension of $10 \times 10 \times 8$ mm. These specimens were homogenized at the temperature range of 480 °C–520 °C in steps of 10 °C for 24 h, respectively. Then the specimens were homogenized at optimized temperature, for 8–24 h in steps of 4 h, respectively. The homogenized samples were quenched into 25 °C water.

The specimens for observation were prepared through conventional metallographic procedures and followed by etching in a standard Keller's reagent. Then the specimens were observed by Leica DIM 3000 optical microscope and JSM-6510 scanning electron microscope (SEM). The transition points of as-cast alloy 2618 were measured from 300 °C to 800 °C with differential scanning calorimeter (DSC) at a heating rate of 5 °C/min. The compositions of main constituent phases of alloy 2618 were analyzed by energy dispersive X-ray analyzer attached to the SEM.

3 Result and discussion

3.1 As-cast microstructure of alloy 2618

The most commonly secondary phases observed in as-cast alloy 2618 are S (Al_2CuMg) and Al_9FeNi phase, although, a small quantity of AlNiCu or AlCuFe phase would exist because of the componential fluctuation in casting alloy [9, 22]. Fig. 1 shows the microstructure of as-cast alloy 2618 prepared by conventional DC casting in present study. A large amount of secondary phases precipitated along the grain boundaries owing to severe dendritic segregation clearly shown in Fig. 1(b). The typical dendritic α (Al) matrix phase can be observed in Fig. 1(a) and needle-like Al_9FeNi phase exists at the grain boundaries and stretches into the grains. Table 2 displays the compositions of secondary phases at grain boundary of as-cast alloy 2618. According to the EDS-X-ray analysis, the white and clear-boundary structure including tiny black spots is perceived as non-equilibrium α–Al + θ (Al_2Cu) eutectic structure (spot A in Fig. 1(b)) instead of typical α–Al + S (Al_2CuMg). The white and bright phase with fuzzy bound-

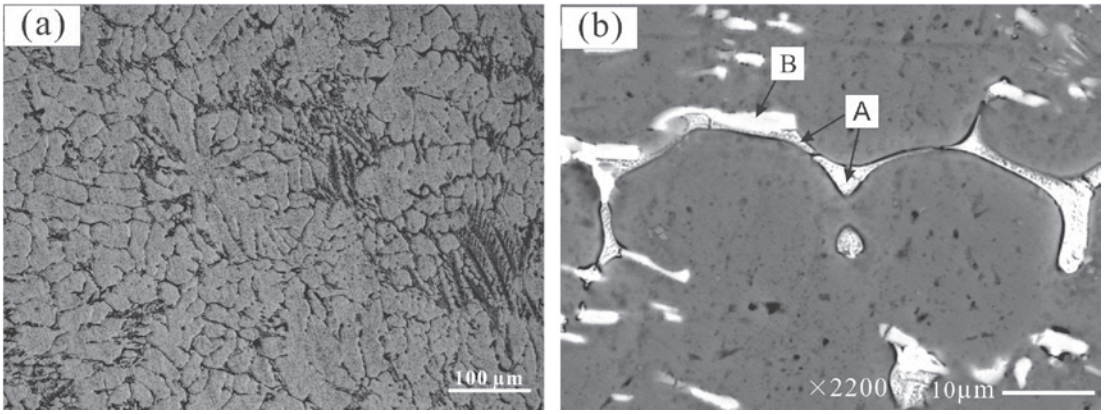

Fig. 1: Microstructure of as-cast alloy 2618 prepared by conventional DC casting

Table 2: Compositions of secondary phases at grain boundary of as-cast alloy 2618 (in at.%).

Analysis spot	Al	Cu	Mg	Fe	Ni
A	68.62	29.04	1.32	0.21	0.81
B	83.39	1.03	1.02	6.77	7.63

ary is regarded as Al_9FeNi (spot B in Fig. 1(b)). Since some incident electron beams of EDS would penetrate into aluminum matrix to a certain extent, which could lead to higher content of Al and a small amount of Cu and Mg in spot B.

The SEM microstructure and the distributions of elements Al, Cu, Mg, Fe and Ni in as-cast alloy 2618 are shown in Fig. 2. It can be seen that elements Cu, Fe and Ni are enriched in grain boundaries and Al as solvent element is

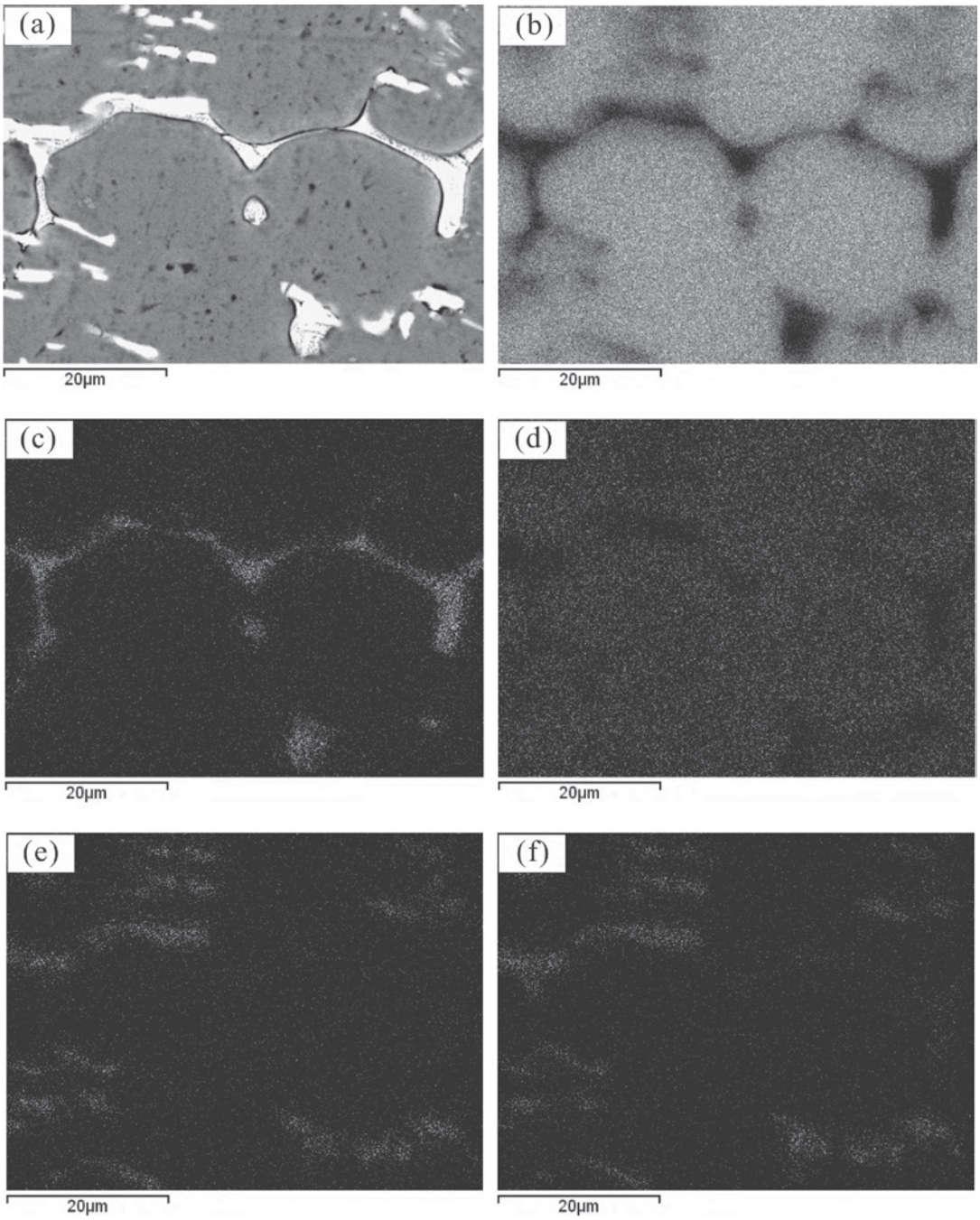

Fig. 2: SEM microstructure of as-cast alloy 2618 and elements distribution: (a) SEM microstucture; (b) Al; (c) Cu; (d) Mg; (e) Fe; (f) Ni

lacking in grain boundaries. But it is very interesting to find that Mg as a solute element is also lacking in grain boundaries rather than enriched in the form of secondary phase S (Al_2CuMg), which is in accordance with above EDS analysis. This phenomenon can be explained using Al-Mg and Al-Cu binary phase diagrams and the non-equilibrium solidification owing to the rapid cooling rate of the as-cast samples in the present experiment. The maximal solubilitys of Mg and Cu in Al at their eutectic temperatures of 450 °C and 548.2 °C are 17.2 mass% and 5.7 mass%, respectively. The rapid cooling of the as-cast samples and the higher solubility of Mg in Al solid solution lead to the decreased precipitation tendency of Al_2CuMg. The higher eutectic temperature of Al-Cu alloy results in the preferential precipitation of θ (Al_2Cu) phase. Additionally, the average content of Mg in alloy 2618 is only 1.6 mass%, which brings about the solubility gradient required for diffusion is small. Consequently, the element Mg could not precipitate in the form of S (Al_2CuMg) phase in alloy 2618 of present experiment. So element Mg still solves in Al matrix with a slight degree of supersaturation at room temperature. The segregation degree of solute elements in grain boundaries is Cu > Fe ≈ Ni > Mg. Therefore, homogenization treatment is very necessary to eliminate severe dendritic segregation in as-cast alloy 2618. Generally, the relationship between diffusion coefficient and the temperature can be expressed by Arrhenius equation as:

$$D = D_0 \exp\left(-\frac{Q}{RT}\right) \tag{1}$$

where D_0 is the diffusion constant, R the mole gas constant, Q the diffusion activation energy and T is the absolute temperature. The diffusion velocity of atoms increases with the increase of temperature and diffusion constant, which is in favor of eliminating severe dendritic segregation in as-cast alloy. Thus, the homogenization temperature should be selected as higher as possible to accelerate the homogenization process. Yet, in order to avoid the overburning of alloy, the temperature should be below a certain value, which will be discussed in the next section.

3.2 Homogenized microstructure of alloy 2618

3.2.1 Effect of homogenization temperature on microstructure

Fig. 3 shows the optical microstructure of as-cast alloy 2618 and the alloys homogenized at different temperatures for 24 h, respectively. Typical dendritic crystals with some residual phases at interdendritic region were observed in Fig. 3(a). The non-equilibrium θ phases existed in eutectic structures were dissolved into the matrix at different temperatures with different extents during homogenization process. The higher the homogenization temperature, the more complete the homogenization of alloy 2618 is (see Fig. 3(b)–(d)). The θ phase distributed continuously along grain boundaries in as-cast alloy as shown in Fig. 3(a). After homogenization at 480 °C for 24 h (see Fig. 3(b)), most of non-equilibrium θ phases dissolved in matrix. As shown in Fig. 3(c) and (d), the eutectic structures with low-melting point were almost dissolved into the matrix completely and the dendritic network structure disappeared. When the homogenization temperature increased to 510 °C, slight overburning occurred at grain boundaries. A few spherical and triangular structures formed as shown in Fig. 3(e). When homogenization at 520 °C, severe overburnt structures could be observed as shown in Fig. 3(f). Besides, the morphology of Al_9FeNi phase turned from needle-like to spherality and the phase became coarse when the alloy was homogenized at 510–520 °C. So, the appropriate homogenization temperature is 500 °C.

3.2.2 Effect of homogenization time on microstructure

Fig. 4 presents the SEM microstructure of as-cast alloy 2618 and the alloys homogenized at 500 °C for different times. Continuous network eutectic structures existed in the grain boundaries could be observed in Fig. 4(a). With the increase of holding time, the continuous network eutectic structures were broken and the volume fraction of residual phases at grain boundaries reduced gradually as shown in Fig. 4(b)–(f). It can be seen in Fig. 4(d) that the volume fraction of residual phases in alloy 2618 was the least after homogenization at 500 °C for 16 h. Besides, the size and morphology of Al_9FeNi phase had little change. With the further increase of homogenization time, there was no obvious change in matrix microstructure of alloy 2618 as shown in Fig. 4(e) and Fig. 4(f), except slight coarsing of Al_9FeNi phase. As a result, the suitable homogenization parameters for alloy 2618 based on present studies are: homogenized at 500 °C for 16 h.

3.3 DSC and line scanning analysis for as-cast and homogenized alloy 2618

Fig. 5 gives the DSC curves of as-cast alloy 2618 and the alloy homogenized at 500 °C for 16 h. Two endothermic

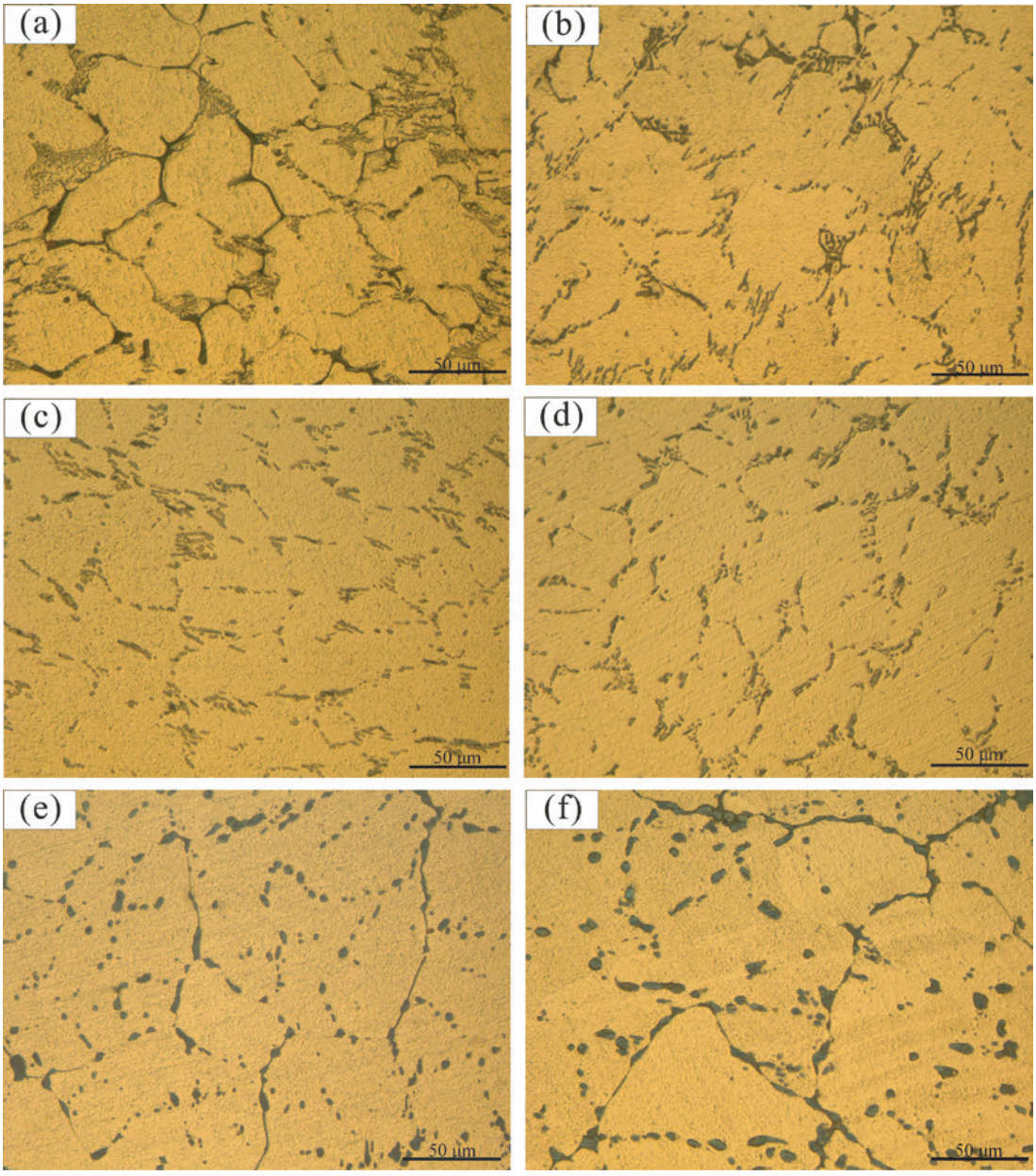

Fig. 3: Optical microstructure of as-cast alloy 2618 and the alloys homogenized at different temperatures for 24 h, respectively: (a) as-cast; (b) 480 °C; (c) 490 °C; (d) 500 °C; (e) 510 °C; (f) 520 °C

peaks are observed in as-cast alloy, sited at 506.4 °C and 638 °C, respectively. After the alloy was homogenized at 500 °C for 16 h, the endothermic peak at 506.4 °C disappeared. The transition temperature corresponds to the fusion temperature of non-equilibrium eutectic structures, which is generally called the overburnt temperature of the alloy. The transition temperature 638 °C is identified as the liquidus temperature of the as-cast alloy. So the homogenization temperature should not surpass 506.4 °C in order to avoid the overburning of alloy 2618, which is in good accordance with experimental results obtained in homogenization process. After homogenization, the liquidus temperature of alloy shifted to 641 °C as shown in Fig. 5. This phenomenon could be explained as follows. When liquid alloy 2618 solidified at higher cooling rate, there existed a larger degree of supercooling. The homogenized alloy 2618 could be regarded as the alloy 2618 solidified at very slow cooling rate. At this process, there is almost no supercooling. So, when the as-cast alloy 2618 was reheated, the liquidus temperature would be lower than that of the homogenized alloy, too.

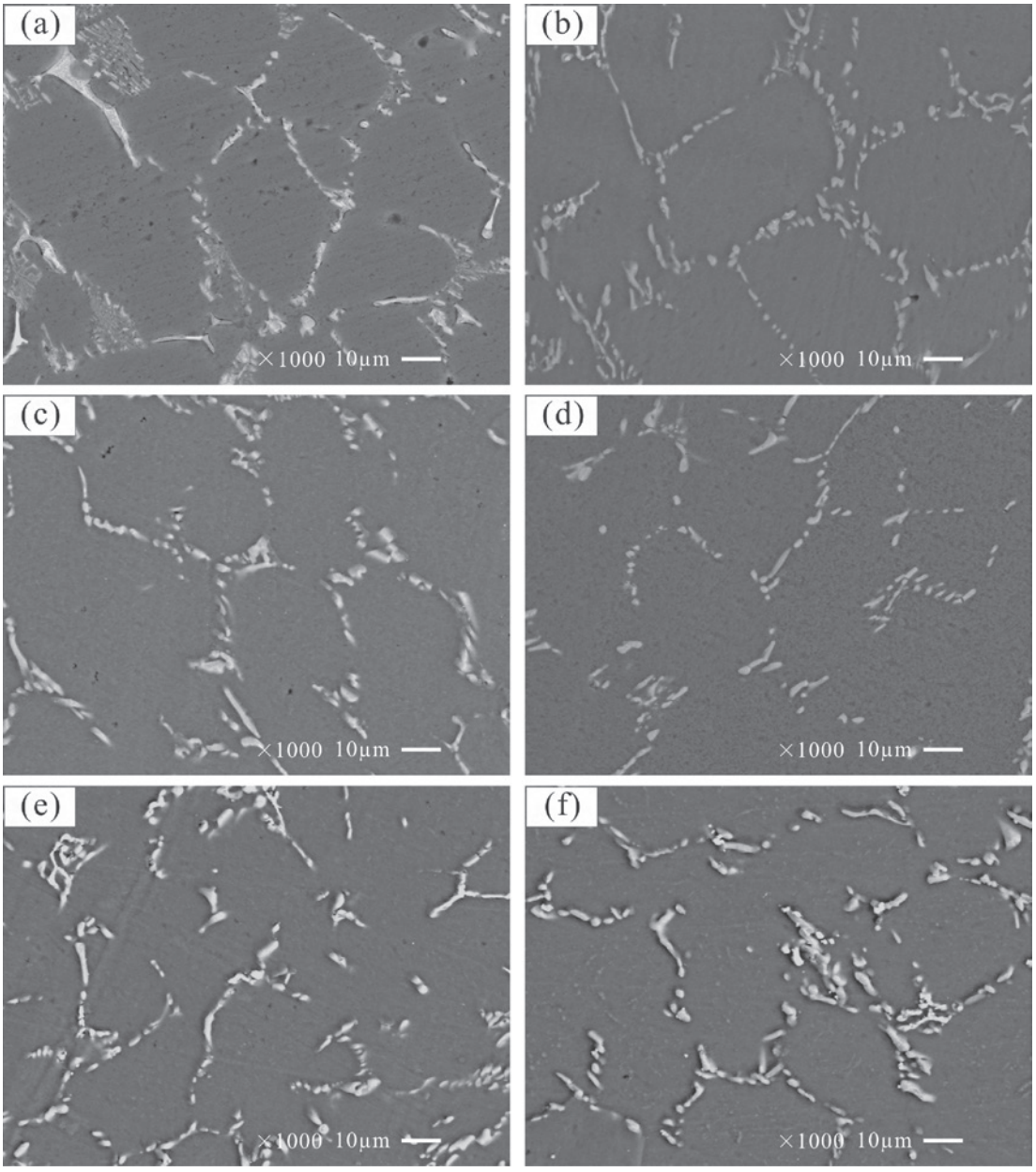

Fig. 4: SEM microstructure of as-cast alloy 2618 and the alloys homogenized at 500 °C for different times: (a) as-cast; (b) 8 h; (c) 12 h; (d) 16 h; (e) 20 h; (f) 24 h

The increase of liquidus temperature after homogenization results from the higher concentration of alloying elements excluding Mg in α (Al) matrix. It can be conclude that the homogenization temperature should not surpass the overburnt temperature of 506.4 °C, which is in good accordance with experimental results obtained in homogenization process.

Fig. 6 gives the line-scan analysis results of main alloying elements in alloy 2618 before and after homogenization at 500 °C for 16 h. It can be seen that the distribution of elements Cu, Mg, Fe and Ni at and near grain boundaries are heterogeneous in as-cast alloy and distribute periodically as shown in Fig. 6(a). Elements Cu, Fe and Ni segregate seriously at grain boundaries and decrease remarkably away from grain boundaries in as-cast alloy. While element Mg is poor in grain boundaries and its content increases remarkably away from grain boundaries. Within grains, the content of all elements are homogeneous as shown in Fig. 6(a). After homogenization, the segregation of Cu at grain boundaries is reduced dramatically and

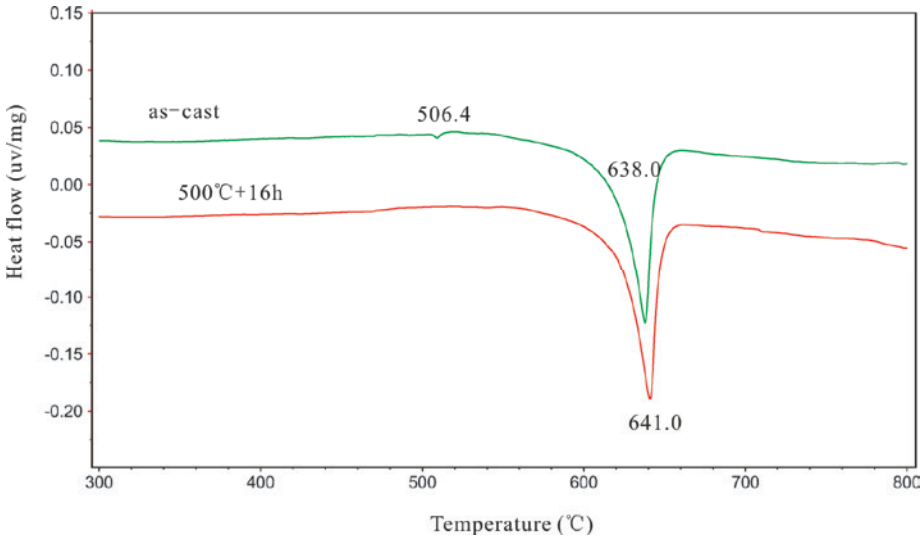

Fig. 5: DSC curves of as-cast alloy 2618 and the alloy homogenized at 500 °C for 16 h

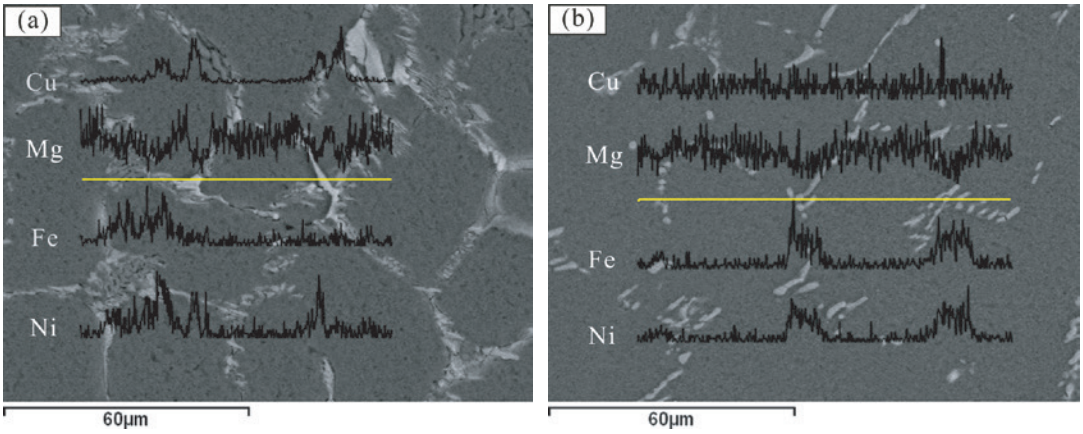

Fig. 6: Line-scan analysis of elements in alloy 2618 before and after homogenization: (a) as-cast; (b) homogenized at 500 °C for 16 h

the distribution of Mg in interdendritic region becomes more even, compared with as–cast alloy. The segregations of Fe and Ni still exist with few changes as shown in Fig. 6(b), which can be ascribed to the existence of Al_9FeNi phase in grain boundaries. It was reported that even though alloy 2618 was homogenized at 640 °C for 24 h, the Al_9FeNi phase still could not be dissolved entirely in matrix [23]. Additionally, slight segregation of Cu still existed in homogenization aluminum alloys due to lower diffusion coefficient of Cu [16, 21, 24] and the same result is also found in this paper. Thus, the homogenized process of alloy 2618 is mainly controlled by the diffusion of element Cu.

3.4 Kinetic analysis for homogenization of alloy 2618

The investigation on distribution of main solute elements at interdendritic region in alloy 2618 is very useful to the design of homogenization process. Based on the analysis of Shewmon [25], the initial distribution of solute element

along interdendritic region can be approached by Fourier series component in a cosine function as:

$$C(x) = \bar{C} + A_0 \cos\frac{2\pi x}{L} \tag{2}$$

$$A_0 = \frac{1}{2}(C_{\max} - C_{\min}) = \frac{1}{2}\Delta C_0 \tag{3}$$

where $\bar{C}$ is the average concentration of solute element, L the interdendritic spacing, A_0 the initial amplitude of the composition segregation, χ the distance of a certain position away from the grain boundaries and ΔC_0 is the concentration difference of the solute element between grain boundary and grain inside. Fig. 7 illustrates the distribution of solute element during homogenization according to Eq. (2) and Eq. (3). It can be concluded that amplitude of composition segregation decreases with the increase of homogenization time. Every fundamental wave component of the elemental distribution approached by Eq. (2) would decay with the increase of the homogenization time, which can be expressed in the decay function of fundamental wave as [26]:

$$C(x,t) = \bar{C} + \frac{1}{2}\Delta C_0 \cos\left(\frac{2\pi x}{L}\right)\exp\left(-\frac{4\pi^2}{L^2}Dt\right) \tag{4}$$

Eq. (4) can also be represented by decay function as:

$$C(x,t) = \frac{1}{2}\Delta C_0 \exp\left(-\frac{4\pi^2}{L^2}Dt\right) \tag{5}$$

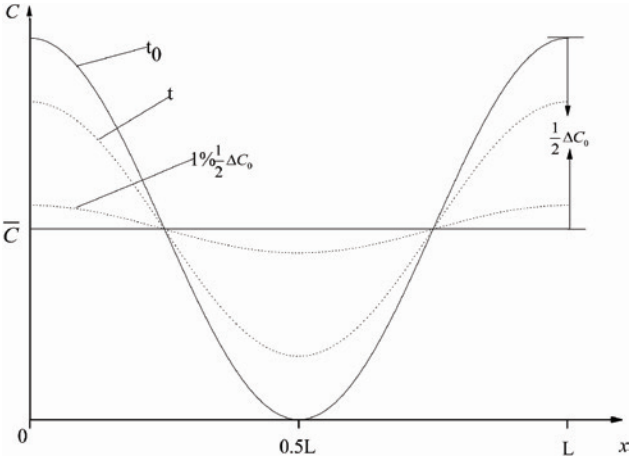

Fig. 7: Scheme of the distribution of solute element during homogenization

where D is the diffusion coefficient, considering the diffusion coefficient is susceptible to temperature, substitute Eq. (1) into Eq. (5), the equation can be rewritten as:

$$C(x,t) = \frac{1}{2}\Delta C_0 \exp\left[-\frac{4\pi^2 D_0 t}{L^2}\exp\left(-\frac{Q}{RT}\right)\right] \tag{6}$$

It can be concluded from Eq. (6) that elemental segregation at interdendritic regions can be removed by prolonging the holding time (t) or increasing the homogenized temperature (T), which is accordant with the experimental results.

The complete uniform distribution of solute element in alloy is too hard to reach during homogenization. So the element distribution could be identified as uniform distribution if the composition segregation amplitude (A_0) decreases to $\delta \cdot A_0$, as calculated using Eq. (7).

$$\delta \cdot A_0 = \frac{1}{2}\Delta C_0 \exp\left[-\frac{4\pi^2 D_0 t}{L^2}\exp\left(-\frac{Q}{RT}\right)\right] \tag{7}$$

By taking natural logarithms of both sides, Eq. (8) can be finally obtained as:

$$\frac{1}{T} = \frac{R}{Q}\ln\left(-\frac{4\pi^2 D_0 t}{L^2 \ln\delta}\right) \tag{8}$$

Assume $A = R/Q$ and $B = -4\pi^2 D_0 / \ln\delta$, Eq. (8) can be rewritten as:

$$\frac{1}{T} = A\ln\left(\frac{Bt}{L^2}\right) \tag{9}$$

Eq. (9) is the final kinetic equation for homogenization. Both A and B are constant, which can be calculated using the existing data [16] of $D_0(\mathrm{Cu}) = 0.084$ cm^2/s, $Q(\mathrm{Cu}) = 136.8$ KJ/mol and $R = 8.31$ J/(mol·K). So the homogenization kinetic curves of alloy 2618 can be obtained as shown in Fig. 8 and the recommended value of δ is 1/100 [16].

It can be seen from Fig. 8 that the homogenization time will be shorten dramatically by increasing homogenization temperature at the same interdendritic spacing, which is credited to the higher diffusion rate of atoms at high temperature. Moreover, the homogenization time decreases sharply with the decrease of interdendritic spacing at the same temperature. The smaller the interdendritic spacing is, the higher the segregation decaying rate is.

The average interdendritic spacing L of alloy 2618 in present experiment is about 46 μm based on quantitative

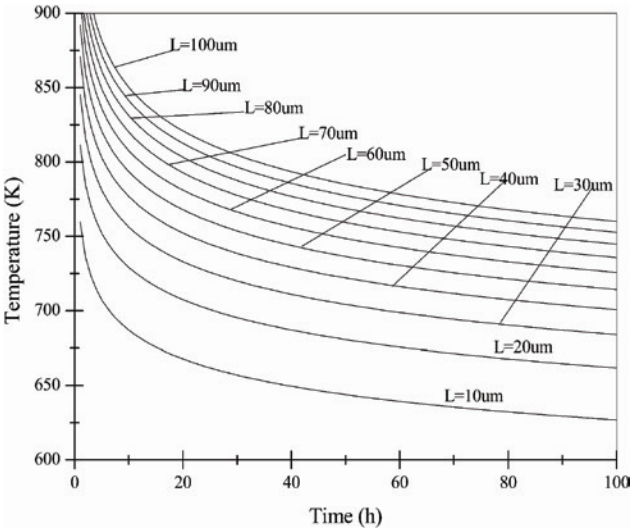

Fig. 8: Relationship between homogenization temperature and time at different interdendritic spacing

metallographic analysis. According to the kinetic calculation, the required homogenization time for alloy 2618 is about 15 h at the optimized homogenization temperature (500 °C), which is well consistent with the experimental results.

4 Conclusions

1. The main constituent phases in as-cast alloy 2618 are dendritic α–Al, needle-like Al_9FeNi and non-equilibrium binary phase θ (Al_2Cu) due to the existence of severe dendritic segregation in as-cast alloy 2618.
2. The overburnt temperature and liquidus temperature of alloy 2618 are 506.4 °C and 638.0 °C, respectively and the optimized homogenization parameters for alloy 2618 are 500 °C for 16 h. After homogenization, the segregation of Cu at grain boundaries in alloy 2618 is reduced dramatically and the liquidus temperature of alloy 2618 shifts to 641 °C.
3. Kinetic analysis for homogenization of alloy 2618 shows that the required homogenization time for the alloy is about 15 h at 500 °C, which is well consistent with that obtained in homogenization experiments.

Acknowledgments: This work was supported by a grant from National Natural Science Foundation of China (no. 51074030) and Qinglan Project.

Received: March 19, 2013. Accepted: April 13, 2013.

References

[1] I. N. A. Oguocha, S. Yannacopoulos and Y. Jin, The structure of Al_xFeNi phase in Al-Cu-Mg-Fe-Ni, *J. Mater. Sci.*, Vol. 31 (1996), 5615–5621.
[2] J. H. Wang, D. Q. Yi and X. P. Su, et al., Influence of deformation ageing treatment on microstructure and properties of aluminum alloy 2618, *Mater. Charact.* Vol. 59 (2008), 965–968.
[3] Z. W. Du, G. J. Wang and X. L. Han, et al., Microstructural evolution after creep in aluminum alloy 2618, *J. Mater. Sci.*, Vol. 47 (2012), 2541–2547.
[4] I. N. A. Oguocha and S. Yannacopoulos, Precipitation and dissolution kinetics in Al-Cu-Mg-Fe-Ni alloy 2618 and Al-alumina particle metal matrix composite, *Mater. Sci. Eng. A*, Vol. 231 (1997), 25–33.
[5] K. Yu, S. R. Li and W. X. Li, Recrystallization behavior in an Al-Cu-Mg-Fe-Ni alloy with trace scandium and zirconium, *Mater. Trans.*, 41, No. 2 (2000), 358–361.
[6] K. Yu, W. X. Li and S. R. Li, Mechanical properties and microstructure of aluminum alloy 2618 with Al_3(Sc, Zr) phases, *Mater. Sci. Eng. A*, Vol. 368 (2004), 88–93.
[7] J. H. Wang and D. Q. Yi, Preparation and Properties of Alloy 2618 Reinforced by Submicron AlN Particles, *J. Mater. Eng. Perform.*, 15, No. 5 (2006), 596–600.
[8] F. Bardi, M. Cabibbo and S. Spigarelli, An analysis of thermo-mechanical treatments of a 2618 aluminium alloy study of optimum conditions for warm forging, *Mater. Sci. Eng. A*, Vol. 334 (2002), 87–95.
[9] F. Nový, M. Janeček and R. Král, Microstructure changes in a 2618 aluminium alloy during ageing and creep, *J. Alloys. Compd.*, Vol. 487 (2009), 146–151.
[10] K. Yu, S. R. Li and W. X. Li, Effect of Trace Sc and Zr on the Mechanical Properties and Microstructure of Al Alloy 2618, *J. Mater. Sci. Technol.*, 16, No. 4 (2000), 416–420.
[11] K. T. Kashyap, Effect of zirconium addition on the recrystallization behaviour of a commercial Al-Cu-Mg alloy, *Bull. Mater. Sci.*, 24, No. 6 (2001), 643–648.
[12] B. Y. Zong and B. Derby, Creep behavior of a SiC particulate reinforced al-2618 metrix composite, *Acta. Mater.*, 45, No. 1 (1997), 41–49.
[13] F. Ji, M. Z. Ma and A. J. Song, et al., Creep behavior of in situ TiCP/2618 aluminum matrix composite, *Mater. Sci. Eng. A*, Vol. 506 (2009), 58–62.
[14] P. Cavaliere, Mechanical properties of Friction Stir Processed 2618/Al_2O_3/20p metal matrix composite, *Compos. A*, Vol. 36 (2005), 1657–1665.
[15] J. H. Wang, D. Q. Yi and B. Wang, Microstructure and properties of 2618-Ti heat resistant aluminum alloy, *Trans. Nonferr. Met. Soc., China,* 13, No. 3 (2003), 590–594.
[16] X. Y. Liu, Q. L. Pan and X. Fan, et al., Microstructural evolution of Al-Cu-Mg-Ag alloy during homogenization, *J. Alloys. Compd.*, Vol. 484 (2009), 790–794.
[17] G. R. Purdy and J. S. Kirkaldy, Homogenization by diffusion, *Metall. Mater. Trans. B*, Vol. 2 (1971), 371–378.
[18] G. S. Cole, Inhomogeneities and their control via solidification, *Metall. Mater. Trans. B*, Vol. 2 (1971), 357–370.
[19] L. M. Wu, W. H. Wang and Y. F. Hsu, et al., Effects of homogenization treatment on recrystallization behavior and

dispersoid distribution in an Al-Zn-Mg-Sc-Zr alloy, *J. Alloys. Compd.*, Vol. 456 (2008), 163–169.

[20] L. Z. He, X. H. Li and X. T. Liu, et al., Effects of homogenization on microstructures and properties of a new type Al-Mg-Mn-Zr-Ti-Er alloy, *Mater. Sci. Eng. A*, Vol. 527 (2010), 7510–7518.

[21] W. B. Li, Q. L. Pan and Y. P. Xiao, et al., Microstructural evolution of ultra-high strength Al-Zn-Cu-Mg-Zr alloy containing Sc during homogenization, *Trans. Nonferr. Met. Soc., China*, Vol. 21 (2011), 2127–2133.

[22] J. H. Wang and D. Y. Yi, Effect of melt over-heating and Zr alloying on the morphology of Al_9FeNi phase and mechanical propreties of 2618 alloy, *Acta. Metall. Sin., (English Letters)*, 15, No. 6 (2002), 525–530.

[23] İ. Özbek, A study on the re-solution heat treatment of AA 2618 aluminum alloy, *Mater. Charact.*, Vol. 58 (2007), 312–317.

[24] C. L. Li, Q. L. Pan and X. Y. Liu, et al., Homogenizing heat treatment of 2124 aluminum alloy, *Chin. J. Nonferr. Met.*, 20, No. 2 (2010), 209–216.

[25] P. G. Shewmon, Diffusion in Solids, Second ed., McGraw Hill, New York (1963).

[26] X. T. Liu and J. Z. Cui, Study on the Diffusion Kinetics Of Aluminum Alloy Cast during Homogenizing Treatment, *Mater. Rev.*, 18, No. 6 (2004), 102–104.